ISSN 1948-9358 (online)

World Journal of *Diabetes*

World J Diabetes 2024 September 15; 15(9): 1829-2001

Published by Baishideng Publishing Group Inc

World Journal of Diabetes

Contents

Monthly Volume 15 Number 9 September 15, 2024

EDITORIAL

FIELD OF VISION

REVIEW

MINIREVIEWS

ORIGINAL ARTICLE

Case Control Study

World Journal of Diabetes

Monthly Volume 15 Number 9 September 15, 2024

Contents

World Journal of Diabetes

Monthly Volume 15 Number 9 September 15, 2024

Contents

NAME OF JOURNAL
World Journal of Diabetes

ISSN
ISSN 1948-9358 (online)

LAUNCH DATE
June 15, 2010

FREQUENCY
Monthly

EDITORS-IN-CHIEF
Lu Cai, Md. Shahidul Islam, Michael Horowitz

EDITORIAL BOARD MEMBERS
https://www.wjgnet.com/1948-9358/editorialboard.htm

PUBLICATION DATE
September 15, 2024

INSTRUCTIONS TO AUTHORS
https://www.wjgnet.com/bpg/gerinfo/204

GUIDELINES FOR ETHICS DOCUMENTS
https://www.wjgnet.com/bpg/GerInfo/287

GUIDELINES FOR NON-NATIVE SPEAKERS OF ENGLISH
https://www.wjgnet.com/bpg/gerinfo/240

PUBLICATION ETHICS
https://www.wjgnet.com/bpg/GerInfo/288

PUBLICATION MISCONDUCT
https://www.wjgnet.com/bpg/gerinfo/208

ARTICLE PROCESSING CHARGE
https://www.wjgnet.com/bpg/gerinfo/242

STEPS FOR SUBMITTING MANUSCRIPTS
https://www.wjgnet.com/bpg/GerInfo/239

ONLINE SUBMISSION
https://www.f6publishing.com

World Journal of Diabetes

Submit a Manuscript: https://www.f6publishing.com

World J Diabetes 2024 September 15; 15(9): 1942-1961

DOI: 10.4239/wjd.v15.i9.1942

ISSN 1948-9358 (online)

ORIGINAL ARTICLE

Basic Study

Molecular mechanisms of Buqing granule for the treatment of diabetic retinopathy: Network pharmacology analysis and experimental validation

Yi-Fan Yang, Ling Yuan, Xiang-Yang Li, Qian Liu, Wen-Jie Jiang, Tai-Qiang Jiao, Jia-Qing Li, Meng-Yi Ye, Yang Niu, Yi Nan

Specialty type: Endocrinology and metabolism

Provenance and peer review: Unsolicited article; Externally peer reviewed.

Peer-review model: Single blind

Peer-review report's classification

Scientific Quality: Grade A, Grade C, Grade C

Novelty: Grade B, Grade B

Creativity or Innovation: Grade B, Grade B

Scientific Significance: Grade A, Grade B

P-Reviewer: Ebraheim LLM; Horowitz M; Tatmatsu-Rocha JC

Received: April 12, 2024

Revised: July 5, 2024

Accepted: July 31, 2024

Published online: September 15, 2024

Processing time: 137 Days and 7.8 Hours

Yi-Fan Yang, Wen-Jie Jiang, Jia-Qing Li, Yang Niu, Yi Nan, Key Laboratory of Ningxia Minority Medicine Modernization Ministry of Education, Ningxia Medical University, Yinchuan 750004, Ningxia Hui Autonomous Region, China

Ling Yuan, College of Pharmacy, Ningxia Medical University, Yinchuan 750004, Ningxia Hui Autonomous Region, China

Xiang-Yang Li, Tai-Qiang Jiao, Meng-Yi Ye, Yang Niu, Traditional Chinese Medicine College, Ningxia Medical University, Yinchuan 750004, Ningxia Hui Autonomous Region, China

Qian Liu, School of Clinical Medicine, Ningxia Medical University, Yinchuan 750004, Ningxia Hui Autonomous Region, China

Co-corresponding authors: Yang Niu and Yi Nan.

Corresponding author: Yi Nan, MD, Professor, Key Laboratory of Ningxia Minority Medicine Modernization Ministry of Education, Ningxia Medical University, No. 1160 Shengli Street, Yinchuan 750004, Ningxia Hui Autonomous Region, China. 20080011@nxmu.edu.cn

Abstract

BACKGROUND

Diabetic retinopathy (DR) is a common microvascular complication of diabetes mellitus. Its blindness rate is high; therefore, finding a reasonable and safe treatment plan to prevent and control DR is crucial. Currently, there are abundant and diverse research results on the treatment of DR by Chinese medicine Traditional Chinese medicine compounds are potentially advantageous for DR prevention and treatment because of its safe and effective therapeutic effects.

AIM

To investigate the effects of Buqing granule (BQKL) on DR and its mechanism from a systemic perspective and at the molecular level by combining network pharmacology and *in vivo* experiments.

METHODS

This study collected information on the drug targets of BQKL and the therapeutic

targets of DR for intersecting target gene analysis and protein-protein interactions (PPI), identified various biological pathways related to DR treatment by BQKL through Gene Ontology and Kyoto Encyclopedia of Genes and Genomes enrichment analyses, and preliminarily validated the screened core targets by molecular docking. Furthermore, we constructed a diabetic rat model with a high-fat and high-sugar diet and intraperitoneal streptozotocin injection, and administered the appropriate drugs for 12 weeks after the model was successfully induced. Body mass and fasting blood glucose and lipid levels were measured, and pathological changes in retinal tissue were detected by hematoxylin and eosin staining. ELISA was used to detect the oxidative stress index expression in serum and retinal tissue, and immunohistochemistry, real-time quantitative reverse transcription PCR, and western blotting were used to verify the changes in the expression of core targets.

RESULTS

Six potential therapeutic targets of BQKL for DR treatment, including Caspase-3, c-Jun, TP53, AKT1, MAPK1, and MAPK3, were screened using PPI. Enrichment analysis indicated that the MAPK signaling pathway might be the core target pathway of BQKL in DR treatment. Molecular docking prediction indicated that BQKL stably bound to these core targets. *In vivo* experiments have shown that compared with those in the Control group, rats in the Model group had statistically significant ($P < 0.05$) severe retinal histopathological damage; elevated blood glucose, lipid, and malondialdehyde (MDA) levels; increased Caspase-3, c-Jun, and TP53 protein expression; and reduced superoxide dismutase (SOD) and glutathione peroxidase (GSH-Px) levels, ganglion cell number, AKT1, MAPK1, and MAPK3 protein expression. Compared with the Model group, BQKL group had reduced histopathological retinal damage and the expression of blood glucose and lipids, MDA level, Caspase-3, c-Jun and TP53 proteins were reduced, while the expression of SOD, GSH-Px level, the number of ganglion cells, AKT1, MAPK1, and MAPK3 proteins were elevated. These differences were statistically significant ($P < 0.05$).

CONCLUSION

BQKL can delay DR onset and progression by attenuating oxidative stress and inflammatory responses and regulating Caspase-3, c-Jun, TP53, AKT1, MAPK1, and MAPK3 proteins in the MAPK signaling pathway mediates these alterations.

Key Words: Diabetic retinopathy; Network pharmacology; Animal models; Oxidative stress; Inflammatory

Core Tip: In this study, we constructed a diabetic retinopathy (DR) model in Sprague-Dawley rats and combined network pharmacology and *in vivo* experiments to thoroughly investigate the therapeutic efficacy of Buqing granule in DR and their mechanism of action. The experimental data showed that Buqing granule could significantly reduce oxidative stress and inflammatory damage, thus delaying DR. This finding not only deepens our understanding of DR pathogenesis, but also provides new ideas and potential therapeutic targets for future innovation in DR treatment.

Citation: Yang YF, Yuan L, Li XY, Liu Q, Jiang WJ, Jiao TQ, Li JQ, Ye MY, Niu Y, Nan Y. Molecular mechanisms of Buqing granule for the treatment of diabetic retinopathy: Network pharmacology analysis and experimental validation. *World J Diabetes* 2024; 15(9): 1942-1961

URL: https://www.wjgnet.com/1948-9358/full/v15/i9/1942.htm

DOI: https://dx.doi.org/10.4239/wjd.v15.i9.1942

INTRODUCTION

Diabetic retinopathy (DR) is a severe disease that damages the retina due to the effects of prolonged hyperglycemia on the blood vessels and tissues of the eye and requires a high level of attention for patients with diabetes[1]. DR pathogenesis is complex, and its treatment can be challenging. The best option for reducing the risk of retinopathy onset and progression is to control blood glucose, blood pressure, and lipids[2]. The most common clinical treatments include steroids, anti-vascular endothelial growth factor therapy, vitrectomy, and laser therapy[3]. However, these treatment modalities are expensive and may have specific side effects. Therefore, finding treatment modalities that have few adverse effects and are safe and effective in DR should be developed.

Buqing granule (BQKL) are a traditional prescription first described in "Yangshi Jiacang Fang". It tonifies the kidneys, benefits its essence, nourishes the liver, and brightens the eyes. In the preliminary stage of this study, the chemical components of the herbal medicines were qualitatively detected using HPLC-IT-TOF for studying the pharmacological substance basis and quality control of BQKL. In addition, clinical observations and pharmacological experiments found[4,5] that BQKL has excellent antioxidant and hypoglycemic effects and delays ophthalmopathy onset and development in diabetes. However, studies on the pharmacological effects of BQKL in DR treatment and the underlying molecular

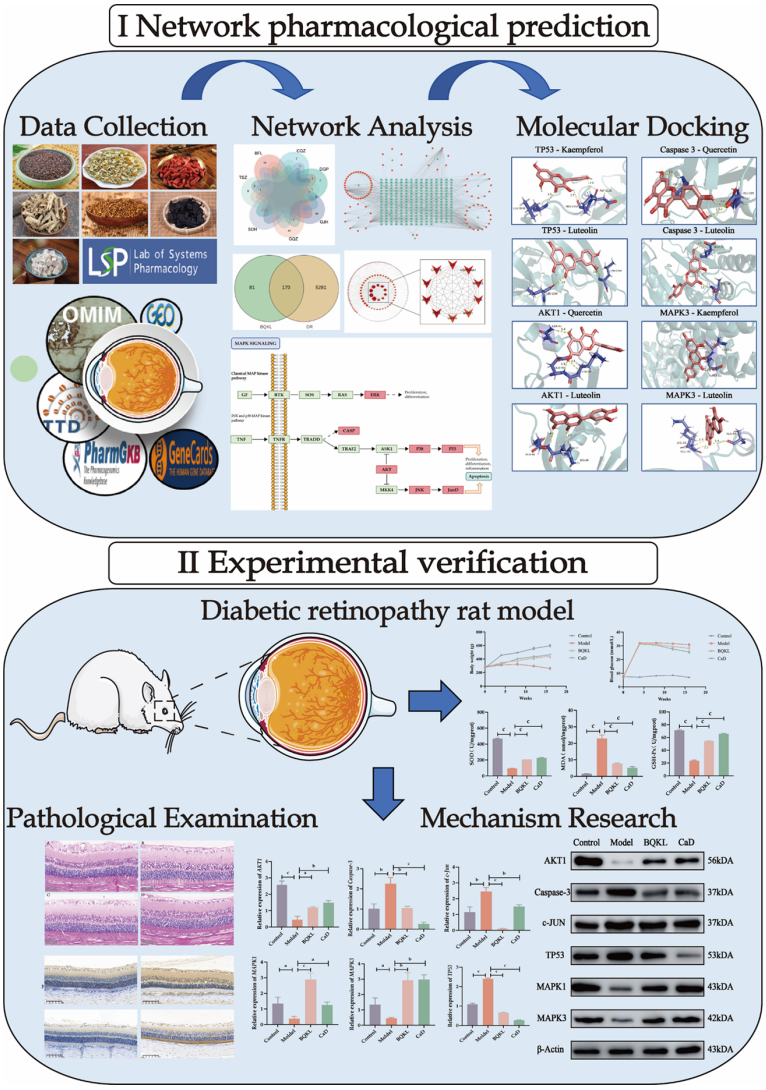

Figure 1 Research flow chart. $^{a}P < 0.05$, $^{b}P < 0.01$, $^{c}P < 0.001$.

mechanisms need to be conducted.

Network pharmacology combines computer science and systems biology to study the mechanism of drug action and molecular design of multitarget drugs[6]. It focuses on exploring "drug-disease-target gene" interaction networks at a systemic and comprehensive level. Chinese medicines and their formulas are characterized by multi-component, multi-pathway, and multi-target synergistic effects, which are advantageous for preventing and treating complex diseases. Network pharmacology has many similarities with the holistic concepts of traditional Chinese medicine, which provide a new perspective and solution for studying the mechanism of action and the material basis of the efficacy of compound formulas of Chinese medicines[7]. This study aimed to explore the potential mechanism by which BQKL treats DR using a combination of network pharmacology and animal experiments and establish a foundation for its future clinical application (Figure 1).

MATERIALS AND METHODS

Screening of the active ingredients in BQKL

The BQKL active ingredients were searched using TCMSP (https://old.tcmsp-e.com/tcmsp.php)[8] to screen the potential targets of action of BQKL. The potential targets of active ingredients were supplemented by PubMed (https://pubmed.ncbi.nlm.nih.gov/). A network diagram of "BQKL-Active Ingredients-Targets of Action" was constructed.

DR-related target prediction

GeneCards[9] (https://www.genecards.org/), OMIM[10] (https://omim.org/), TTD[11] (http://db.idrblab.net/ttd/), PharmGKB[12] (https://www.pharmgkb.org/) combined with GEO[13] (http://www.ncbi.nlm.nih.gov/geo/) and other databases were searched to collect, merge, and de-emphasize disease targets to identify potential DR targets.

Venn diagram and protein-protein interaction network construction

InteractiVenn[14] (http://www.interactivenn.net/index2.html) mapped the screened disease targets to the BQKL compound targets, and the intersecting targets were considered the targets of action of the BQKL for treating DR. The intersected targets were imported into the STRING database[15] (https://cn.string-db.org/) for protein interaction information. Cytoscape 3.9.0 was used for visualization, free target removal, protein-protein interaction (PPI) network construction, network topology analysis, and the degree value of the targets in the PPI network calculation.

GO and KEGG enrichment analyses

Overlapping intersection targets were added to the DAVID database[16] (https://david.ncifcrf.gov/tools.jsp), and GO and KEGG enrichment analyses were performed. The results were visualized using an online tool (https://www.bioinformatics.com.cn) and Adobe Illustrator 2020.

Molecular docking

The SDF structure files of the core BQKL compounds were downloaded from Pubchem[17] (https://pubchem.ncbi.nlm.nih.gov/). High-resolution PDB format files of the BQKL core compound genes were obtained from the PDB database[18] (https://www.rcsb.org) and processed using PyMOL 2.5.2 for dehydrogenation and hydrogenation after deletion of the proto-ligands contained in the large-molecule receptors. The processed large and small molecules were imported into AutoDockTools 1.5.7 for molecular docking verification, and the docking results were visualized using PyMOL 2.5.2.

Animals

Five-week-old male Sprague-Dawley rats, body mass (220 ± 20) g, were purchased from the Animal Experiment Center of Ningxia Medical University, acclimatized for one week, and observed daily. During the experimental period, the rats had access to sufficient water and food; the bedding in the cages was changed daily to keep them dry, ensure animal welfare, and strictly implement ethical animal requirements. All animal experiments were approved by the Laboratory Animal Welfare Ethics Committee of Ningxia Medical University Laboratory Animal Center (No. IACUC-NYLAC-2022-113).

Drug preparation

All herbs used in this study were purchased from the Traditional Chinese Medicine Hospital of Ningxia Medical University and prepared according to standards. BQKL comprises *Cuscuta chinensis* Lam. (*C. chinensis* Lam.) (Tusizi) 20 g, *Lycium barbarum* L. (*L. barbarum* L.) (Gouqizi) 20 g, *Lycium chinense* Mill. (*L. chinense* Mill.) (Digupi) 10 g, *Plantago asiatica* L. (*P. asiatica* L.) (Cheqianzi) 10 g, *Chrysanthemum morifolium* Ramat. (*C. morifolium* Ramat.) (Ganjuhua) 10 g, *Rehmannia glutinosa* Libosch. (*R. glutinosa* Libosch.) (Shudihuang) 20 g, and *Poria cocos* (Schw.) Wolf [*P. cocos* (Schw.) Wolf] (Baifuling) 20 g. The positive control drug Calcium Dobesilate (CaD) was purchased from Ningxia Kangya Pharmaceutical Co.

Establishment of a rat model of DR

After 1 week of acclimatization, the rats were randomly divided into blank control and model groups. The blank group was fed normal chow, and the model group was fed high-fat and high-sugar chow[19] (Boaigang-1135DM, Beijing Boai Port Biotechnology Co., Ltd., China). After 4 weeks, all the rats were fasted for 12 hours. The rats in the model group were intraperitoneally injected with 60 mg/kg streptozotocin (STZ, Boaigang-B2001, Beijing Boai Port Biotechnology Co. Ltd., China) to induce diabetes mellitus. Eight rats in the blank control group were intraperitoneally injected with the same volume of sodium citrate buffer. A model was established if the random fasting blood glucose level was higher than 16.7 mmol/L after 72 hours[20]. After successful modeling, the model group rats were divided into model, BQKL, and CaD groups with eight rats in each group. For 12 weeks, rats in the BQKL[21] and CaD[22] groups received 800 and 104 mg/kg/day medication, respectively, by gavage, and rats in the control and model groups received an equal amount of physiological saline. During the experiments, we paid full attention to and minimized the pain and discomfort of the experimental animals. To reduce the pain of experimental rats, we chose to euthanize rats by carbon dioxide asphyxiation.

Body weight and blood glucose measurement

The eyeballs, fur color, diet, water intake, urine output, body shape, mental status, and activity were observed and recorded weekly during the experimental period. Body weight and blood glucose were measured at the end of 1 week of acclimatization feeding at 0, 4, 8, 12, and 16 weeks for each group of rats, respectively.

Serum biochemical analyses and ELISA tests

Serum total cholesterol (TC) and triglyceride (TG) levels were measured using an automatic biochemical analyzer, and superoxide dismutase (SOD) and glutathione peroxidase (GSH-Px) activity and malondialdehyde (MDA) levels in the serum and retinal tissue were measured strictly according to the instructions of the ELISA kit.

Hematoxylin-eosin staining

The retinal tissues fixed with 4% paraformaldehyde were wax-embedded. The wax blocks were cut into 5 μm tissue sections using a rotatory microtome, routinely deparaffinized, and stained[23]. Four randomly selected sections from each group were observed under a light microscope and representative images were selected for analysis and recording. Retinal thickness and ganglion cell number were calculated using Adobe Photoshop 22.5.1 and ImageJ 1.53e.

Table 1 Primer information

Gene	Sequence	Product length (bp)
TP53	F:5′-GGCTCCGACTATACCACTATCCAC-3′	129
	R:5'GTCCCGTCCCAGAAGATTCCC-3'	
AKT1	F:5′AACTTCTCAGTGGCACAATGTCAG-3′	71
	R:5′CAGCGGATGATGAAGGTGTTGG-3′	
c-Jun	F:5'TCTACGACGATGCCCTCAACG-3'	99
	R:5′GGTTCAAGGTCATGCTCTGCTTC-3′	
Caspase-3	F:5′CGGTATTGAGACAGACAGTGGAAC-3′	90
	R:5′GCGGTAGAGTAAGCATACAGGAAG-3′	
MAPK1	F:5'CTTCCAACCTCCTGCTGAACAC-3'	117
	R:5′GCGTGGCTACATACTCTGTCAAG-3′	
MAPK3	F:5′CGCATCACAGTAGAGGAAGCAC-3′	72
	R:5′CACTGGTTCATCTGTCGGATCATAG-3′	
GAPDH	F:5′-CAAGTTCAACGGCACAGTCAAGG-3′	123
	R:5′-ACATACTCAGCACCAGCATCACC-3′	

Immunohistochemistry

The sections were dewaxed for aqueous and antigenic repair, incubated overnight with primary antibodies, and then with secondary antibodies for 2 hours at room temperature for DAB color development (all primary antibodies were diluted 1:100). After color development, the sections were re-stained with hematoxylin and sealed with neutral gum. Four sections were randomly selected from each group, and at least four 200 × fields of view were randomly selected from each section for photography. Image Pro Plus software (version 6.0) was used to calculate the integrated optical density and area of positive results in each field of view, and the integrated optical density/area was used as the semi-quantitative result of the assay[24].

Antibodies: MAPK3 Antibody (AF0562, Affinity, United States), c-Jun antibody (AF6090, Affinity, United States), Caspase-3 Antibody (AF6311, Affinity, United States), and ERK2 Antibody (DF6032, Affinity, United States).

Real-time quantitative reverse transcription-PCR

Total RNA from the retinal tissue was extracted according to the instructions of the TRIzol kit and reverse transcribed to cDNA according to the manufacturer's instructions. Fluorescent quantitative primers were designed according to the CDS sequences of the resulting sequences and subjected to real-time fluorescent quantitative PCR. The Cycle Threshold (Ct) values were calculated using the $2^{-\Delta\Delta Ct}$ method[25]. The primers were synthesized by Sangon Biotech Co. (Shanghai, China) (Table 1).

Western blotting

The retinal tissue was lysed and homogenized, and the supernatant was centrifuged for 10 minutes. A BCA kit was used to determine the protein content. Samples were separated by SDS-PAGE gel electrophoresis and transferred to a closed membrane for 2 hours. The primary antibody was added and incubated overnight. The membrane was washed thrice and incubated with the corresponding secondary antibody for 2 hours[26]. The color was developed by adding a luminescent solution and analyzing the relative expression levels of proteins using ImageJ 1.53e.

Antibodies: MAPK3 Antibody (AF0562, Affinity, United States); AKT1 Antibody (AF0836, Affinity, United States); c-Jun Antibody (AF6090, Affinity, United States); Caspase-3 Antibody (AF6311, Affinity, United States); ERK2 Antibody (DF6032, Affinity, United States); TP53 Antibody (DF7238, Affinity, United States); β-actin (AF7018, Affinity, United States); Goat anti-rabbit (S0001, Affinity, United States).

Statistical analysis

Data were statistically analyzed using GraphPad Prism 9.5.0 and expressed as mean ± SD. Comparisons between groups were made using one-way analysis of variance (ANOVA); the SNK-q test was used to test the homogeneity of variance, and the independent samples *t*-test was used to test the heterogeneity of variance. $P < 0.05$ was considered statistically significant[27].

RESULTS

Screening of BQKL active ingredients

A total of 11, 2, 45, 9, 13, 15, and 20 chemical constituents of *C. chinensis* Lam., *R. glutinosa* Libosch., *L. barbarum* L., *P. asiatica* L., *L. chinense* Mill., *P. cocos* (Schw.) Wolf, and *C. morifolium* Ramat., respectively, were collected after screening the literature and consulting databases (Figure 2A). The removal of duplicates revealed 97 main active components of BQKL. After combining and eliminating the duplicate target genes linked to the acquired BQKL compounds, 251 drug targets were identified. Cytoscape 3.9.0 software was used to construct the " BQKL-Active Ingredients-Targets of Action" network (Figure 2B).

BQKL active ingredient screening for the treatment of DR-related targets

By searching the above disease databases, 5451 relevant targets were obtained after merging and de-emphasizing. The BQKL target genes intersected with the DR target, and 170 intersecting genes were obtained (Figure 2C).

PPI network analysis of the core targets of BQKL therapy for DR

The results of the STRING database analysis were further analyzed and visualized using Cytoscape 3.9.0 to establish a PPI network. The figure shows that TP53, AKT1, Jun, Caspase-3, MAPK3, and MAPK1 were closely related to other targets (Figure 2D).

GO analysis and KEGG enrichment of core targets for DR treatment with BQKL

GO and KEGG enrichment analyses of 170 BQKL targets for DR treatment revealed that these targets were mainly enriched various entries closely related to the biological processes of cell growth, proliferation, and apoptosis, such as apoptotic process, positive regulation of cell proliferation, negative regulation of the apoptotic process, and inflammatory response (Figure 3A); The KEGG pathway analysis results show that BQKL acts on 170 possible targets of DR, involving 176 related pathways; these targets are mainly enriched in Metabolic pathways, PI3K Akt signaling pathway, AGE-RAGE signaling pathway in diabetic composites, MAPK signaling pathway, and other pathways (Figure 3B). As the core targets were mainly enriched in the MAPK signaling pathway, we considered the MAPK signaling pathway as the core pathway for DR treatment using BQKL and mapped the target genes in the MAPK signaling pathway (Figure 3C).

Molecular docking

Low free energy of the binding of molecules and targets implies stable binding between the ligand and receptor proteins. The results showed that the binding energies of the BQKL chemical components to the key targets were all less than -5.0 kcal/mol, indicating that the five components of BQKL have strong binding to core targets (Table 2). The docking schematic is shown (Figure 4).

Effects of BQKL on general state, body mass, and blood glucose in DR rats

The control group rats exhibited a good mental state, responsive behavior, soft hair, normal diet and water intake, urine and fecal output, and dry bedding throughout the experimental process. The model group rats displayed lethargy, disheveled and yellowish hair, and were prone to depilation. They also showed significantly increased diet and water intake, urine output, and moist bedding material. The treatment group rats showed some improvement compared with the model group rats.

Before modeling, the rats showed no significant differences in body weight or blood glucose levels ($P > 0.05$). After modeling, the body weights of the control group rats increased steadily. In contrast, the body weights of the model group rats increased insignificantly and then decreased to different degrees over time. Meanwhile, the fasting blood glucose levels of the model group rats were elevated. At weeks 8, 12, and 16, fasting blood glucose was still significantly elevated compared with that of the control group rats, and the body weight of the BQKL and CaD group rats increased significantly ($P < 0.05$ or $P < 0.001$, respectively). Fasting blood glucose levels decreased significantly ($P < 0.001$; Table 3 and Figure 5).

Effect of BQKL on lipid levels in rats

The relevant lipid metabolism indices were altered in the diseased rats treated with BQKL or CaD, with significant decreases in TC and TG levels compared to that in the model group rats ($P < 0.05$ or $P < 0.001$; Table 4 and Figure 6A).

Serum and retinal SOD, MDA, and GSH-Px expression levels in rats of each group

Compared with the control group rats, diabetic rats had significantly higher MDA levels and lower SOD and GSH-Px activities in serum and retinal tissues ($P < 0.001$); compared with the model group rats, diabetic rats treated with BQKL or CaD had significantly lower MDA levels and increased SOD and GSH-Px activities in the serum and tissues of diseased rats ($P < 0.01$). Thus, BQKL can alleviate oxidative damage in the retina and serum of diabetic rats to a certain extent, *i.e.*, it has an ameliorating effect on the degree of oxidative stress in diabetic rats (Table 5, Figure 6B and C).

Histopathological and morphological changes in the rat retina

In the control group, the structure of each retinal layer was clear and intact, and the cells in each layer were tightly arranged with a normal morphology. The model group rats had fewer ganglion cells ($P < 0.001$), loose cells in all layers, an unorganized arrangement, and vacuolar changes in the ganglion cell layer than the control group rats. Compared to

Table 2 Molecular docking binding energy

Molecule Name	Binding energy (kcal/mol)					
	TP53	AKT1	Jun	Caspase-3	MAPK3	MAPK1
Quercetin	-7.3	-6.4	-7.9	-7.9	-7.3	-6.4
Kaempferol	-7.1	-6.3	-7.9	-8.1	-7.1	-6.3
Beta-sitosterol	-7.6	-6.1	-7.3	-8.7	-7.6	-6.1
Luteolin	-7.2	-6.5	-8.6	-8.2	-7.2	-6.5
Stigmasterol	-7	-6.9	-7.6	-7	-7	-6.9

Table 3 Body weight and blood sugar change at different time points (n > 3)

Time (week)	Body weight (g)				Blood glucose (mmol/L)			
	Control	Model	BQKL	CaD	Control	Model	BQKL	CaD
0	267.00 ± 4.58	277.67 ± 11.68	273.00 ± 24.25	290.67 ± 14.98	7.50 ± 0.66	7.00 ± 0.70	7.77 ± 1.74	7.60 ± 1.08
4	457.00 ± 10.58	312.00 ± 6.08	346.33 ± 5.51	324.00 ± 25.71	7.17 ± 0.45	32.13 ± 0.21	31.60 ± 0.53	31.33 ± 0.15
8	493.67 ± 9.50	323.00 ± 17.35	376.33 ± 11.06	403.00 ± 4.68	8.20 ± 0.36	32.10 ± 0.26	30.90 ± 0.61	30.47 ± 0.38
12	556.00 ± 18.36	295.67 ± 12.01	413.00 ± 16.37	432.67 ± 14.19	8.50 ± 0.26	31.67 ± 0.55	29.50 ± 1.08	27.73 ± 0.76
16	597.00 ± 18.25	260.33 ± 14.84	443.67 ± 24.58	464.00 ± 10.15	7.00 ± 0.26	30.70 ± 0.90	28.23 ± 0.61	25.47 ± 0.74

BQKL: Buqing granule; CaD: Calcium dobesilate.

Table 4 Effect of Buqing granule on blood lipids in rats (n > 3)

Groups	TC (mmol/L)	TG (mmol/L)
Control	1.76 ± 0.07	1.17 ± 0.05
Model	3.01 ± 0.09	3.17 ± 0.14
BQKL	2.69 ± 0.07	2.74 ± 0.06
CaD	2.50 ± 0.05	1.30 ± 0.06

BQKL: Buqing granule; CaD: Calcium dobesilate; TC: Total cholesterol; TG: Triglyceride.

Table 5 Effect of Buqing granule on oxidative stress in rat retinal tissue and serum (n > 3)

Groups	Retinal tissue			Blood serum		
	SOD (U/mgprot)	MDA (nmol/mgprot)	GSH-Px (U)	SOD (U/mgprot)	MDA (nmol/mgprot)	GSH-Px (U)
Control	467.77 ± 7.50	1.56 ± 0.08	71.15 ± 1.11	547.83 ± 9.27	8.43 ± 0.42	319.44 ± 3.38
Model	95.25 ± 1.41	22.94 ± 2.11	23.55 ± 1.06	347.22 ± 25.72	45.43 ± 0.99	73.80 ± 0.98
BQKL	202.33 ± 1.89	7.69 ± 0.45	54.37 ± 0.67	515.25 ± 11.60	15.41 ± 0.65	179.72 ± 2.58
CaD	228.47 ± 2.19	5.16 ± 0.70	65.88 ± 0.44	530.68 ± 3.93	15.56 ± 0.28	243.94 ± 1.95

BQKL: Buqing granule; CaD: Calcium dobesilate; SOD: Superoxide dismutase; MDA: Malondialdehyde; GSH-Px: Glutathione peroxidase.

those in the model group rats, the retinal thickness increased, the structure of each layer was neatly arranged, the hierarchy was clear, and the number of ganglion cells increased in the BQKL and CaD group rats (P < 0.05 or P < 0.01; Figure 7).

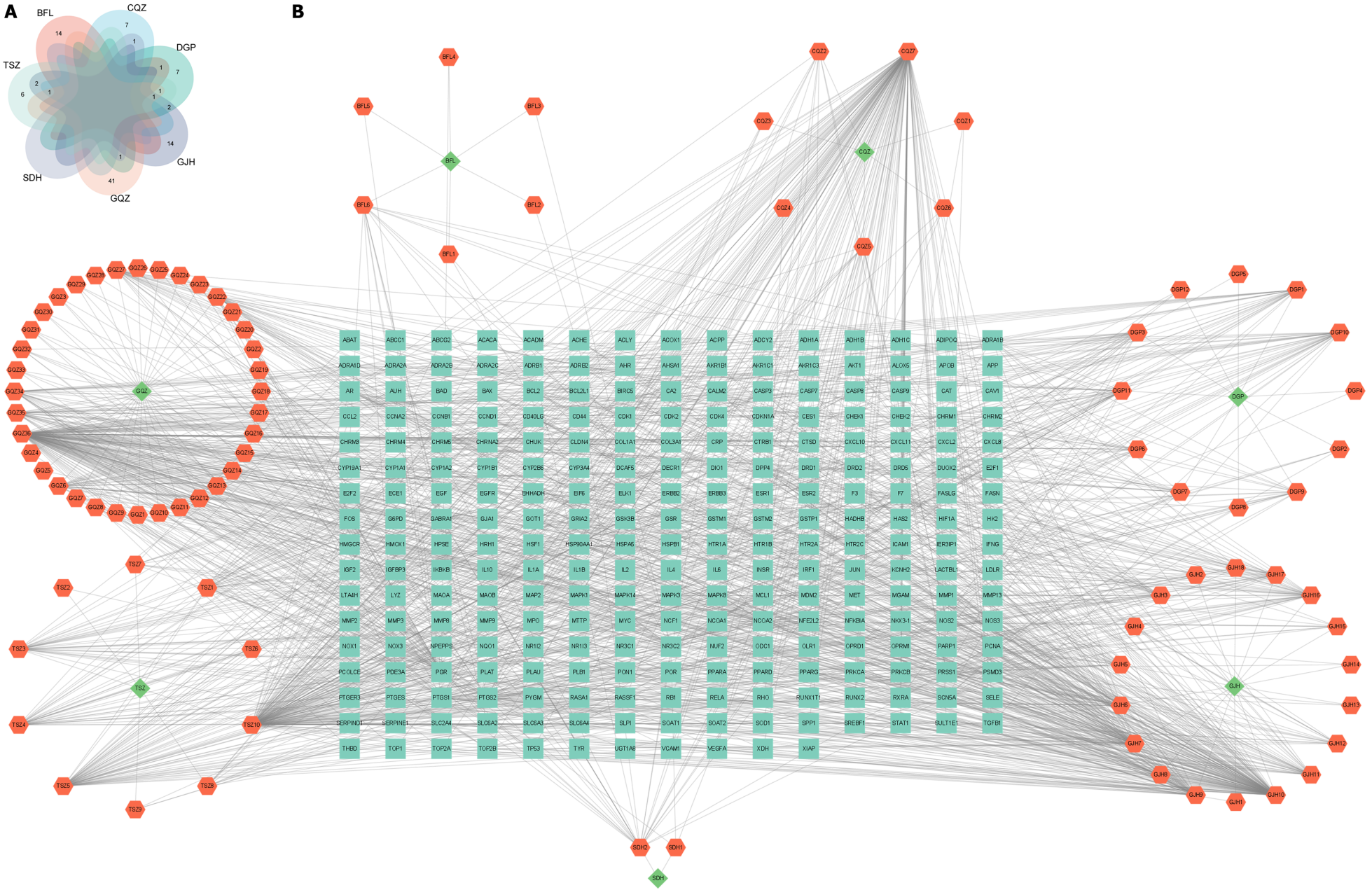
A
BFL
CQZ
DGP
TSZ
GJH
SDH
GQZ
B

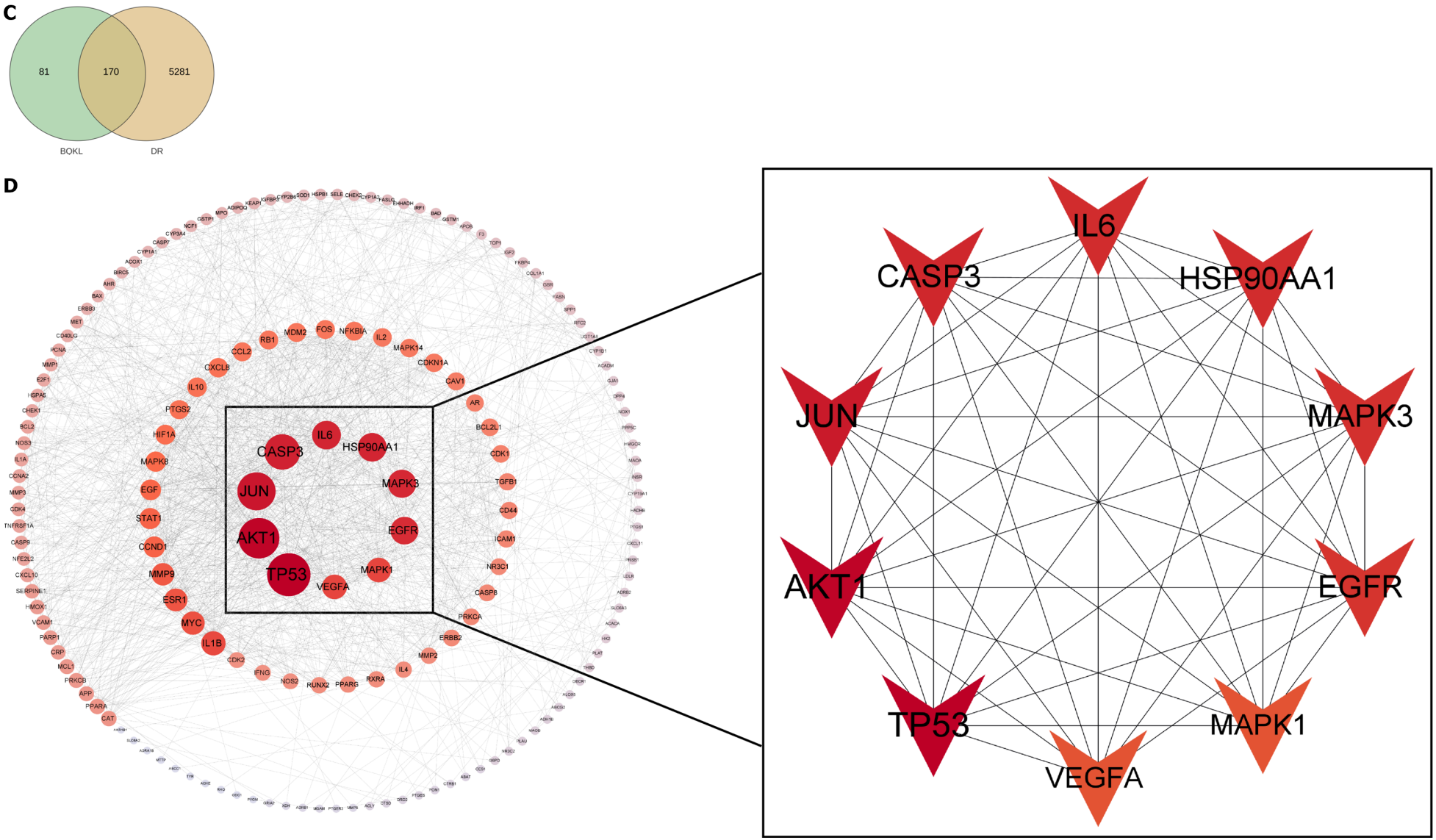

Figure 2 Prediction of diabetic retinopathy components and targets of action of Buqing granule therapy. A: Main ingredients of Buqing granule (BQKL); B: BQKL-active ingredients-targets of action diagram (The rhombus, square hexagon, and square represent the herbal medicine, active ingredient, and target site, respectively); C: Venn diagram of BQKL and diabetic retinopathy (DR) intersection targets; D: Protein-ptrotein interaction network map and screened core BQKL

targets for DR treatment (The darker the color, the larger the icon, the higher the degree value). TSZ: Tusizi; GQZ: Gouqizi; DGP: Digupi; CQZ: Cheqianzi; GJH: Ganjuhua; SDH: Shudihuang; BFL: Baifuling; DR: Diabetic retinopathy; BQKL: Buqing granule.

Immunohistochemical staining of Caspase-3, c-Jun, MAPK1, and MAPK3 in the retinal tissues of rats in each group

The model group rats exhibited significantly higher Caspase-3 and c-Jun expression, and substantially lower MAPK1 and MAPK3 expression, in the retinal tissues than the control group rats ($P < 0.001$). However, both the BQKL and CaD group rats showed decreased Caspase-3 and c-Jun expression ($P < 0.001$), along with elevated MAPK1 and MAPK3 expression ($P < 0.05$ or $P < 0.01$), in the retinal tissues than the model group rats (Figure 8).

Caspase-3, AKT1, c-Jun, TP53, MAPK1, and MAPK3 mRNA expression levels in the retina of rats in each group

Caspase-3, *c-Jun*, and *TP53* mRNA levels in the model group rat retinal tissues were significantly elevated ($P < 0.01$), while *AKT1*, *MAPK1*, and *MAPK3* mRNA levels were significantly decreased ($P < 0.05$), than those in the control group rat retinal tissues. The *Caspase-3*, *c-Jun*, and *TP53* mRNA expressions in the BQKL and CaD group rat retinal tissues were substantially lower than the model group ($P < 0.01$ or $P < 0.001$), whereas *AKT1*, *MAPK1*, and *MAPK3* mRNA expression were significantly higher ($P < 0.05$; Figure 9A).

Caspase-3, AKT1, c-Jun, TP53, MAPK1, and MAPK3 protein expression levels in the retina of rats in each group

Caspase-3, c-Jun, and TP53 protein levels in the model group rats were significantly higher ($P < 0.05$), while AKT1, MAPK1, and MAPK3 levels were significantly lower ($P < 0.05$), than those in the control group rats. However, Caspase-3, c-Jun, and TP53 expression levels in the BQKL and CaD group rat retinal tissues were significantly lower ($P < 0.05$), while AKT1, MAPK1, and MAPK3 expression levels were significantly higher ($P < 0.05$), than those in the control group rats (Figure 9B).

DISCUSSION

With the continuous development of Chinese medicine in recent years, the advantages of traditional Chinese medicine in DR treatment have become increasingly prominent. Several studies have shown that TCM formulas can effectively act together in DR through multiple mechanisms to improve clinical symptoms[28]. This study was primarily based on a network pharmacology approach to explore the potential targets and mechanisms of action of BQKL in DR treatment and experimental validation.

Prolonged hyperglycemia increases protein kinase C, glycated hemoglobin, and polyol metabolite levels, which affect the physiological function of the retina and trigger oxidative stress injury and inflammatory responses. Retinal damage in diabetic rats can be attenuated by its antioxidant and anti-inflammatory properties. In this study, network pharmacology showed that BQKL exerts its anti-DR effects mainly through active compounds such as quercetin, kaempferol, β-sitosterol, lignanserin, and stigmasterol. Quercetin, lignans, and kaempferol belong to the flavonoid family and possess antioxidant, anti-inflammatory, and antitumor properties. Quercetin can improve endothelial function in diabetic rats by inhibiting endoplasmic reticulum stress-mediated oxidative stress[29]; Kahksha *et al*[30] confirmed the antioxidant, anti-diabetic, and anti-inflammatory effects of lignans by showing that the oral administration of lignans could reverse the state of oxidative stress and inflammation in STZ-induced diabetic rats; Alshehri[31] found that kaempferol was rich in targets and could alleviate oxidative stress and inflammation by improving fasting blood glucose and insulin levels in

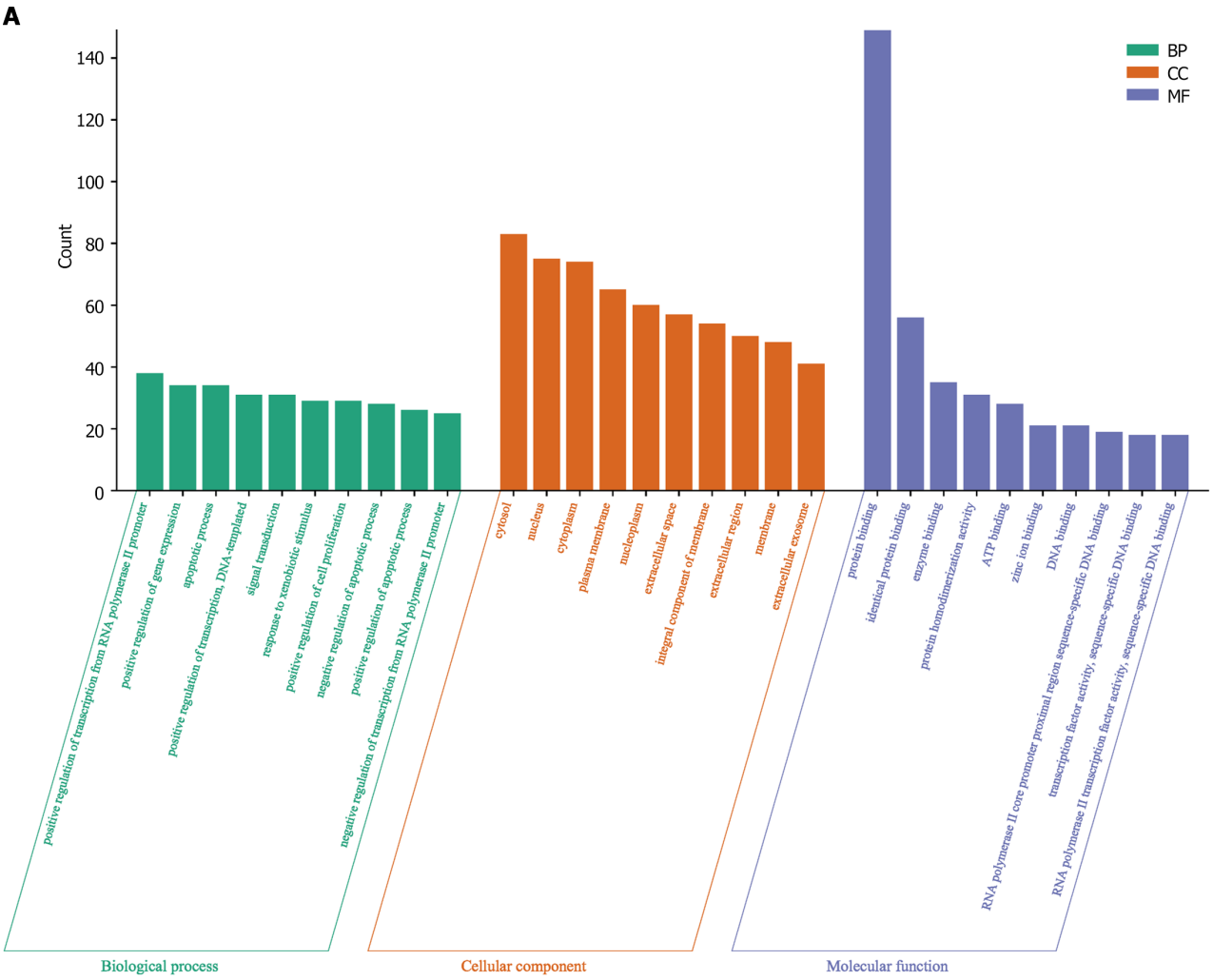
A
BP
CC
MF
Count
0
20
40
60
80
100
120
140
positive regulation of transcription from RNA polymerase II promoter
positive regulation of gene expression
apoptotic process
positive regulation of transcription, DNA-templated
signal transduction
response to xenobiotic stimulus
positive regulation of cell proliferation
negative regulation of apoptotic process
positive regulation of apoptotic process
negative regulation of transcription from RNA polymerase II promoter
cytosol
nucleus
cytoplasm
plasma membrane
nucleoplasm
extracellular space
integral component of membrane
extracellular region
membrane
extracellular exosome
protein binding
identical protein binding
enzyme binding
protein homodimerization activity
ATP binding
zinc ion binding
DNA binding
RNA polymerase II core promoter proximal region sequence-specific DNA binding
transcription factor activity, sequence-specific DNA binding
RNA polymerase II transcription factor activity, sequence-specific DNA binding
Biological process
Cellular component
Molecular function

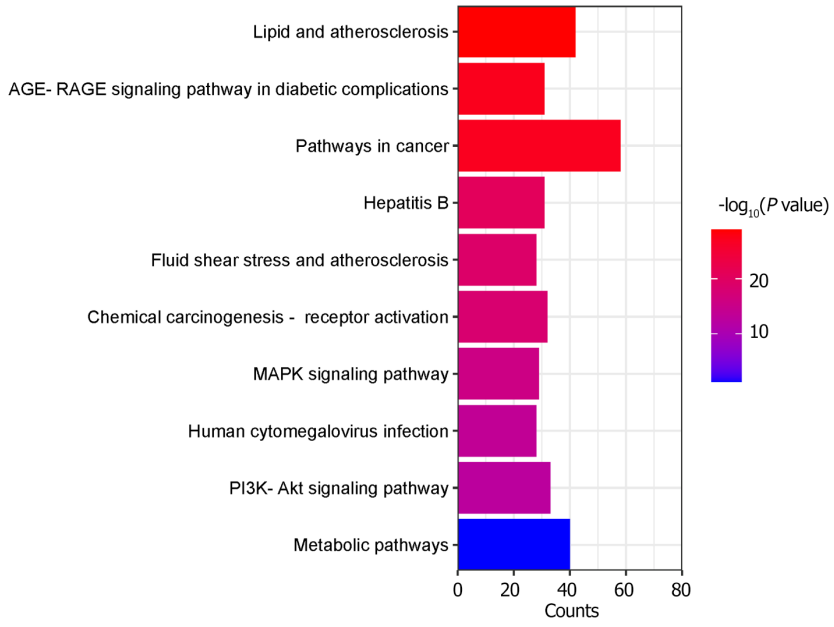
B
Lipid and atherosclerosis
AGE- RAGE signaling pathway in diabetic complications
Pathways in cancer
Hepatitis B
Fluid shear stress and atherosclerosis
Chemical carcinogenesis - receptor activation
MAPK signaling pathway
Human cytomegalovirus infection
PI3K- Akt signaling pathway
Metabolic pathways
0
20
40
60
80
Counts
-log10(P value)
20
10

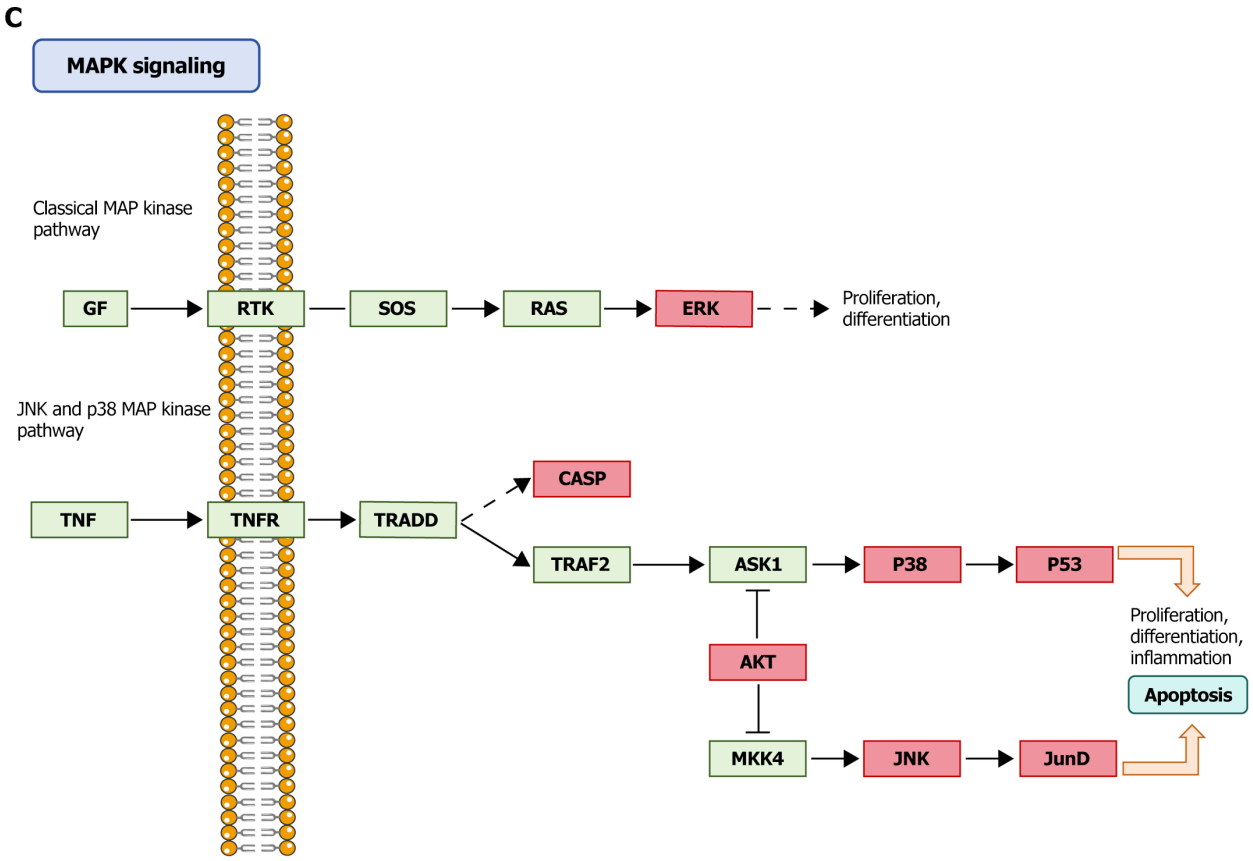

Figure 3 Gene ontology and the Kyoto encyclopedia of genes and genomes enrichment analyses. A: Gene ontology enrichment analysis; B: Kyoto encyclopedia of genes and genomes enrichment analysis; C: Core genes enriched in the MAPK signaling pathway.

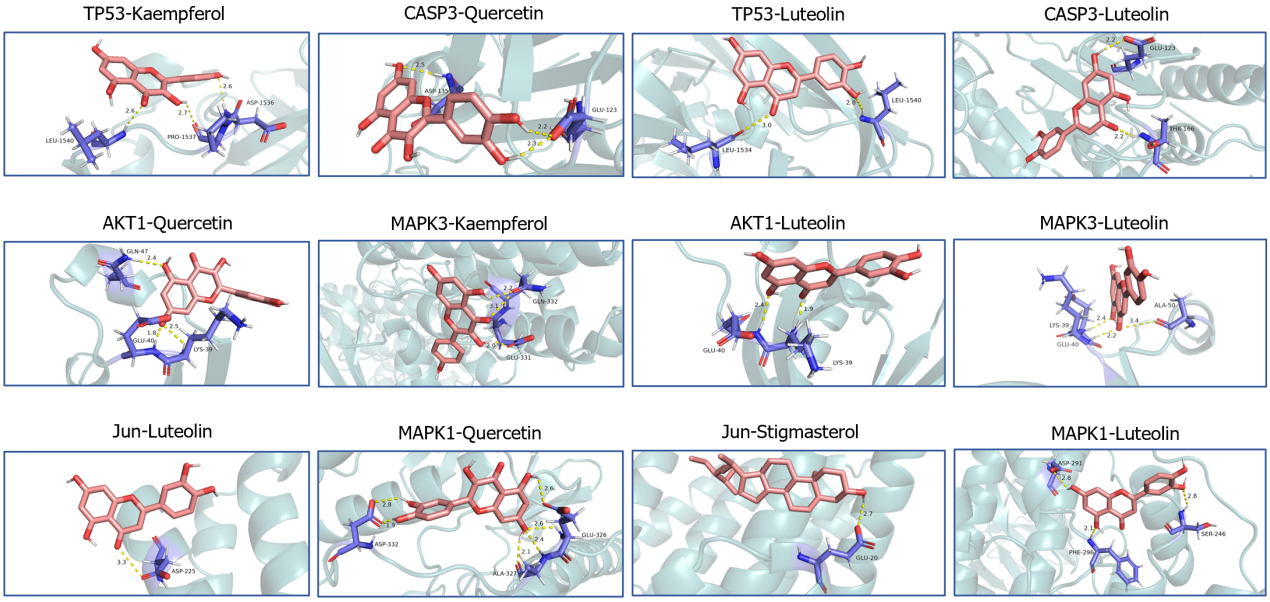

Figure 4 Molecular docking.

diabetic nephropathy rats. Beta-sitosterol and soya sterol are phytosterols, which are not only the primary nutrients of Chinese herbs, but also play a role in lowering lipids by replacing low-density lipoprotein cholesterol in the intestine and interfering with cholesterol absorption because their structure is similar to cholesterol[32]. Babu and Jayaraman[33] found that β-sitosterol could attenuate insulin resistance and mitigate high-fat diet-induced adipose tissue injury by down-regulating the IKKβ/NF-κB and JNK signaling pathways. Wang *et al*[34] found that the possible glucose-lowering mechanism of leguminous stanols is to reduce insulin resistance by enhancing GLUT4 expression and thus regulating the body metabolism. Thus, BQKL is mainly treats DR through flavonoids and phytosterols.

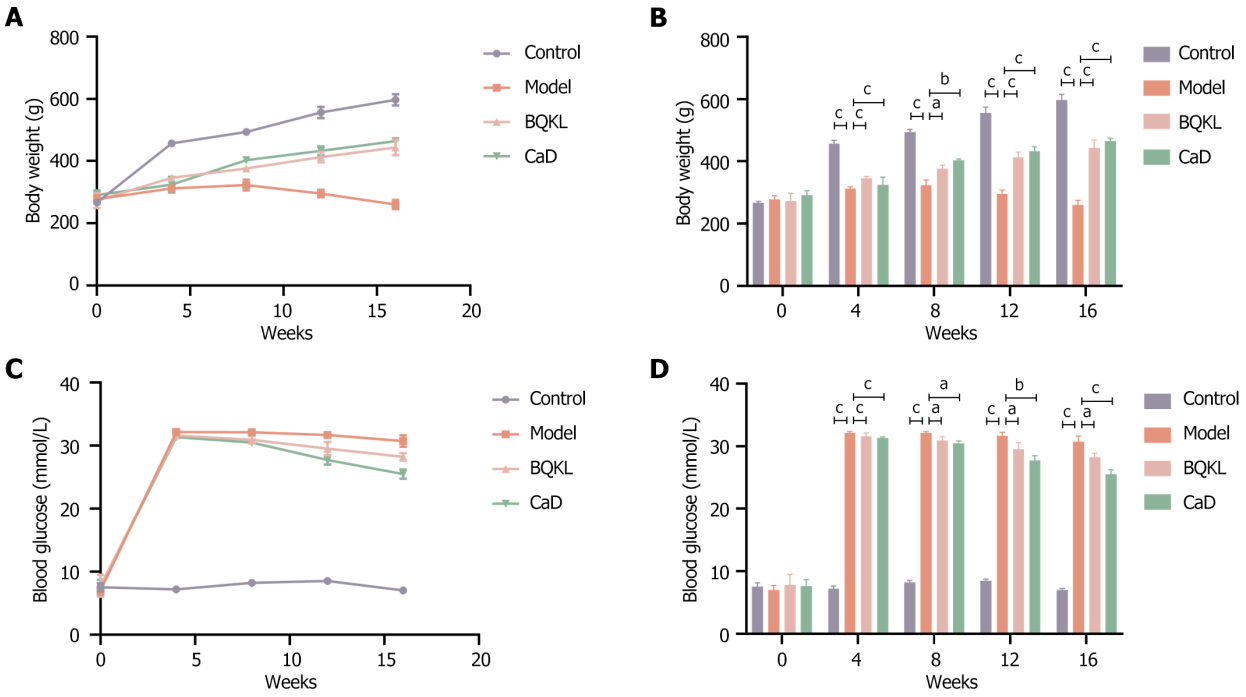

Figure 5 Changes in body weight and blood sugar at different time points. A: Body weight at different time points; B: Blood glucose at different time points. The sequence from left to right represents the control group, the model group, the BQKL group and the CaD group. $^{a}P < 0.05$, $^{b}P < 0.01$, $^{c}P < 0.001$. BQKL: Buqing granule; CaD: Calcium dobesilate.

With the adoption of databases for various diseases, 5451 drug-related targets were obtained after merging and de-emphasizing. Through the construction of a PPI network, 170 potential therapeutic targets closely associated with the treatment of DR with BQKL were identified. The key core targets included TP53, AKT1, Jun, Caspase-3, MAPK3, and MAPK1. A relevant study discovered that excess reactive oxygen species (ROS) production under hyperglycemic conditions can trigger inflammatory responses, mitochondrial dysfunction, and apoptosis, thereby influencing DR onset and progression[35]. Large quantities of p53, an apoptosis-inducing nuclear phosphoprotein, accumulate in the retinal capillaries of diabetic rats. High glucose stimulates p53 accumulation, directly promotes ROS accumulation, and ultimately participates in apoptosis[36]. AKT1 regulates cell proliferation, metabolism, the cell cycle, apoptosis, and inflammatory cell infiltration. A STZ-induced DR mouse model demonstrated that retinal AKT signaling may play a role in maintaining retinal homeostasis. Increased retinal Akt1 activity reduces diabetes-induced molecular changes in the retina[37]. Caspases and Bcl-2 family proteins are the main proteins that regulate apoptosis. When the cells enter the apoptosis program, the expression of the apoptosis-inhibiting protein Bcl-2 and pro-apoptotic protein Bax significantly decreases and increases, respectively, which further amplifies apoptotic signals and stimulates downstream Caspase-3 activation. Once apoptotic signals activate Caspase-3, apoptosis enters an irreversible state. Wu *et al*[38] found, through *in vitro* and *in vivo* experiments, that chrysin significantly decreased the expression of the apoptotic proteins Caspase-3, Caspase-9, and Bax, while increasing the expression of the anti-apoptotic protein Bcl-2 in hyperoside endothelial cells of diabetic rats, thus exerting a protective effect on DR by decreasing oxidative damage and lowering cell damage and apoptosis. Studies have shown[39] that oxidative stress activates the JNK/c-Jun signaling pathway, which is involved in diabetes mellitus development. JNK pathway activation can inhibit insulin secretion while enhancing insulin resistance, resulting in sustained high levels of glucose in the body with consequent enhancement of oxidative stress. Moreover, increased EDEM1 expression blocks the IRE1/JNK/c-Jun signaling pathway, thus elevating insulin mRNA levels. This improvement in insulin secretion normalizes the blood sugar and glucose tolerance levels in diabetic rats. MAPK family kinases are important intracellular signal transduction molecules that affect vascular endothelial cell proliferation, differentiation, and migration by phosphorylating downstream inflammation-associated target genes and regulating biological processes, such as transcription and translation. MAPK1 and MAPK3 inhibition may cause VEGFA-mediated anti-angiogenic effects[40]. Thus, BQKL is a multi-component, multi-target play that delays DR onset and progression.

Functional enrichment analysis further clarified how BQKL acts through critical targets. GO enrichment analysis revealed that the target genes for DR treatment with BQKL were involved in biological processes such as apoptosis and the inflammatory response, which further suggests that BQKL may ameliorate DR through multiple mechanisms. KEGG enrichment analysis showed that BQKL affects various signaling pathways to intervene in DR, among which the MAPK signaling pathway was the most enriched pathway for the core target. Therefore, we inferred that the MAPK signaling pathway is a critical pathway for BQKL to treat DR. The MAPK signaling pathway is regulated by extracellular signal-associated kinases such as ERK and Jun to regulate MAPK, which is involved in various cellular functions, including cell proliferation, differentiation, and migration. According to recent studies, the MAPK signaling pathway plays an essential role in the pathogenesis of diabetic complications. Kuang *et al*[41] found that Qidandihuang decoction improves renal fibrosis in diabetic nephropathy by inhibiting the inflammatory response in diabetic rats *via* the p38MAPK signaling

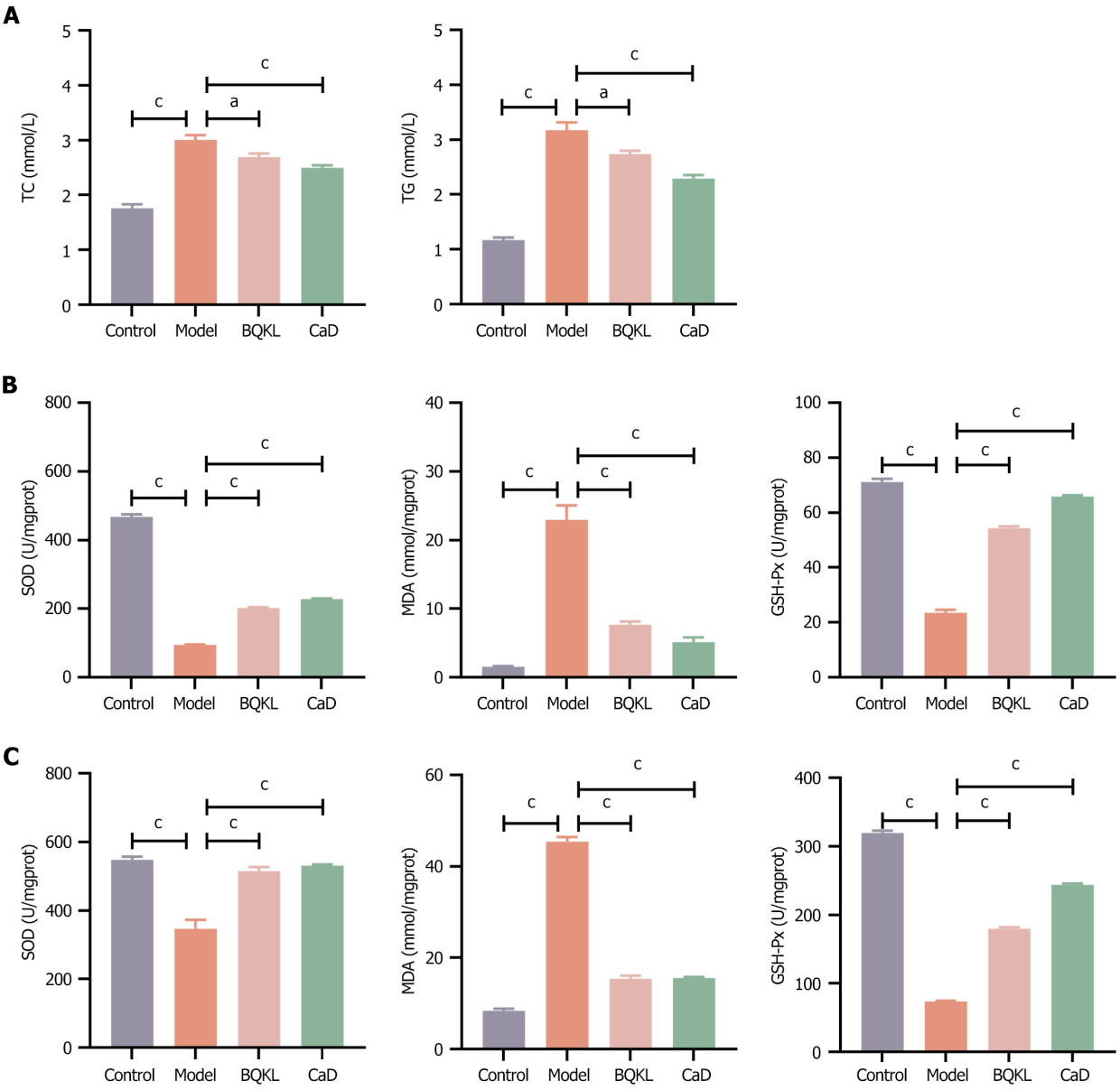

Figure 6 Serum biochemical analyses and ELISA tests. A: Effect of Buqing granule (BQKL) on total cholesterol and triglyceride levels in the serum of diabetic retinopathy (DR) rats; B: Effect of BQKL on superoxide dismutase, malondialdehyde, and glutathione peroxidase contents in the retina of DR rats; C: Effect of BQKL on oxidative stress in rat serum. The sequence from left to right represents the control group, the model group, the BQKL group and the Calcium dobesilate group. $^{a}P < 0.05$, $^{c}P < 0.001$. BQKL: Buqing granule; CaD: Calcium dobesilate.

pathway. Chronic poor glycemic control in patients with diabetes can easily change ocular surface cells, tear composition, osmolarity, and mucin, thus causing diabetic eye diseases, such as dry eye. Chu *et al*[42] found that the MAPK signaling pathway plays a vital role in the pathogenesis of dry eye and the various triggering factors of dry eye increased growth factor levels in the tear fluid and ocular surface tissues, activating the MAPK signaling pathway, which can further increase the levels of inflammatory factors and specific growth factors, thus forming a vicious circle. Blocking MAPK activation at the level of inflammatory factors can improve dry eye symptoms and signs. Wang *et al*[43] found that the expression of pro-inflammatory cytokines was upregulated, MDA content was increased, and SOD and GSH-Px activities were decreased in the retinal tissues in DR rats through a constructed DR rat model, whereas MAPK/NF-κB signaling pathway inhibition ameliorated inflammatory responses and oxidative stress-induced injury, thereby reducing retinal cell apoptosis. Therefore, a protective role of the retina that modulates the MAPK pathway may be an entry point for DR treatment.

In this experiment, the body mass of the model group rat first increased and then decreased, indicating that the model group rats had already entered the late stage of diabetes weight loss in the late stage of the experiment. In contrast, BQKL group rats did not show any symptoms of weight loss, indicating that BQKL could slow the disease process in rats. In addition, fasting blood glucose and blood lipids decreased in rats after BQKL intervention, and the effect of lowering blood glucose and blood lipids was noticeable, indicating an excellent therapeutic effect on diabetes. If the underlying diseases of diabetes can be better controlled, the occurrence of its complication, retinopathy, can also be controlled. Hematoxylin-eosin staining of the retinal tissues of the rats in each group revealed that the retinal thickness of diabetic

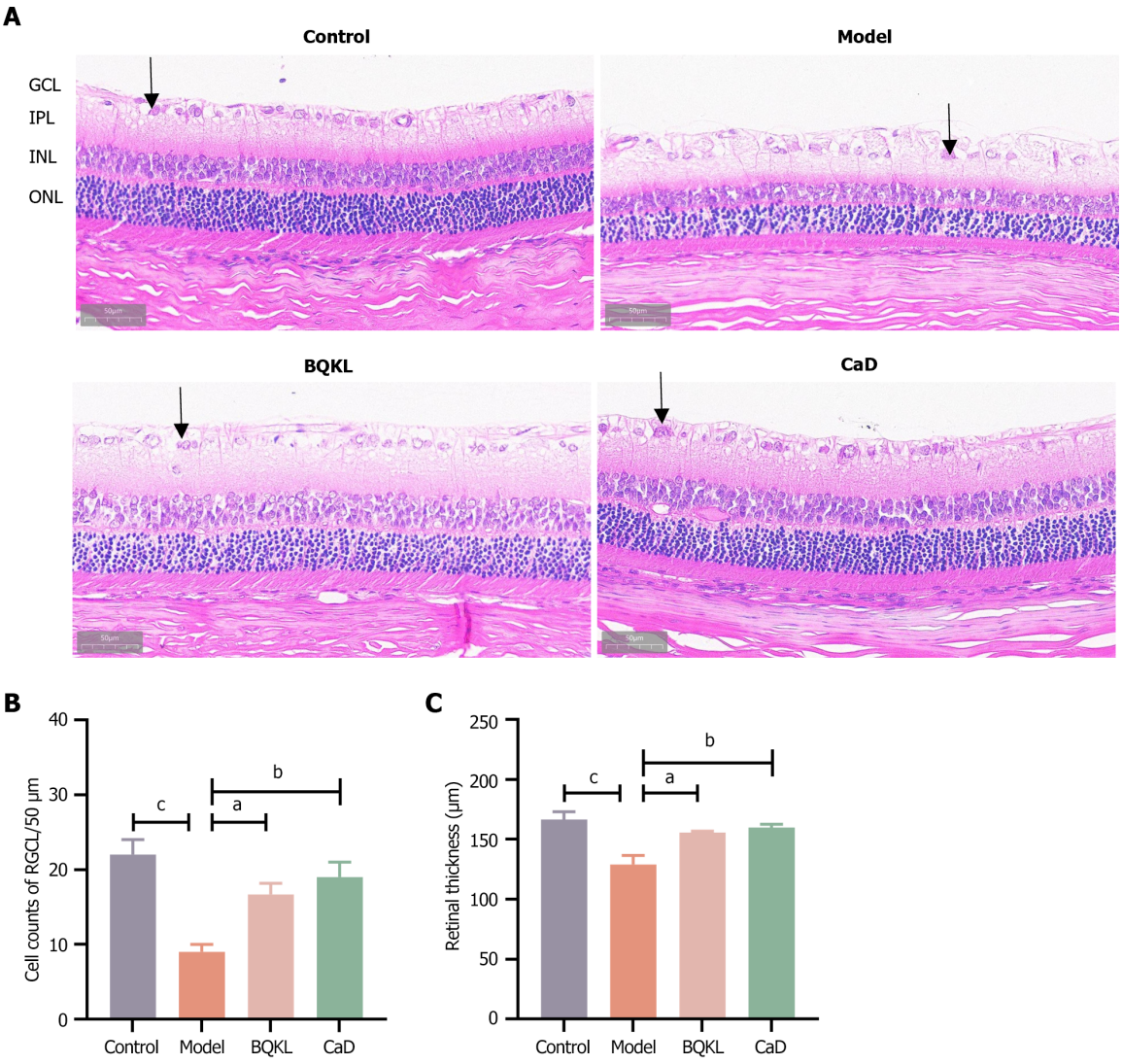

Figure 7 Effects of Buqing granule on retinal morphology in diabetic retinopathy rats. A: Hematoxylin & eosin staining of the retina of rats in each group (400 ×); B: Retinal ganglion cell count in each group; C: Comparison of retinal thickness in each group. The sequence from left to right represents the control group, the model group, the Buqing granule group and the Calcium dobesilate group. $^{a}P < 0.05$, $^{b}P < 0.01$, $^{c}P < 0.001$. BQKL: Buqing granule; CaD: Calcium dobesilate. GCL: Ganglion cell layer; IPL: Inner plexiform layer; INL: Inner nuclear layer; OPL: Outer plexiform layer; ONL: Outer nuclear layer.

rats was reduced, the cells in each layer were loose and disorganized, and the number of ganglion cells was reduced, which improved after BQKL administration. This observation suggests that BQKL partially alleviates retinal pathological changes in diabetic rats.

MDA is a toxic substance produced by the reaction between ROS and lipids and is a significant marker of oxidative stress; SOD and GSH-Px, as essential members of the endogenous antioxidant system, can scavenge various free radicals, including ROS, and maintain the balance between oxidation and antioxidant activity in the organism. Therefore, the MDA content and SOD and GSH-Px activities reflect the oxidative stress degree. This study showed that MDA content significantly increased in the serum and retinal tissues of model group rats. SOD and GSH-Px activities significantly decreased, indicating that the model rats had symptoms of oxidative stress. In contrast, the BQKL group rats showed an inhibited oxidative stress response compared to the model group rats, which indicated that BQKL could improve DR by decreasing the oxidative stress level. In addition, the results of this study showed that the expression of MAPK pathway-related proteins Caspase-3, c-Jun, and TP53 was significantly elevated, while that of AKT1, MAPK1, and MAPK3 proteins were considerably reduced in the model group rats. The elevation of the Caspase-3, c-Jun, and TP53 protein expression was ameliorated and AKT1, MAPK1, and MAPK3 expression improved in the BQKL group rats than that in the model group rats.

CONCLUSION

In summary, BQKL protects against diabetic retinal damage by regulating the expression of relevant proteins in the MAPK signaling pathway, thereby inhibiting oxidative stress and inflammatory responses (Figure 10). However, this

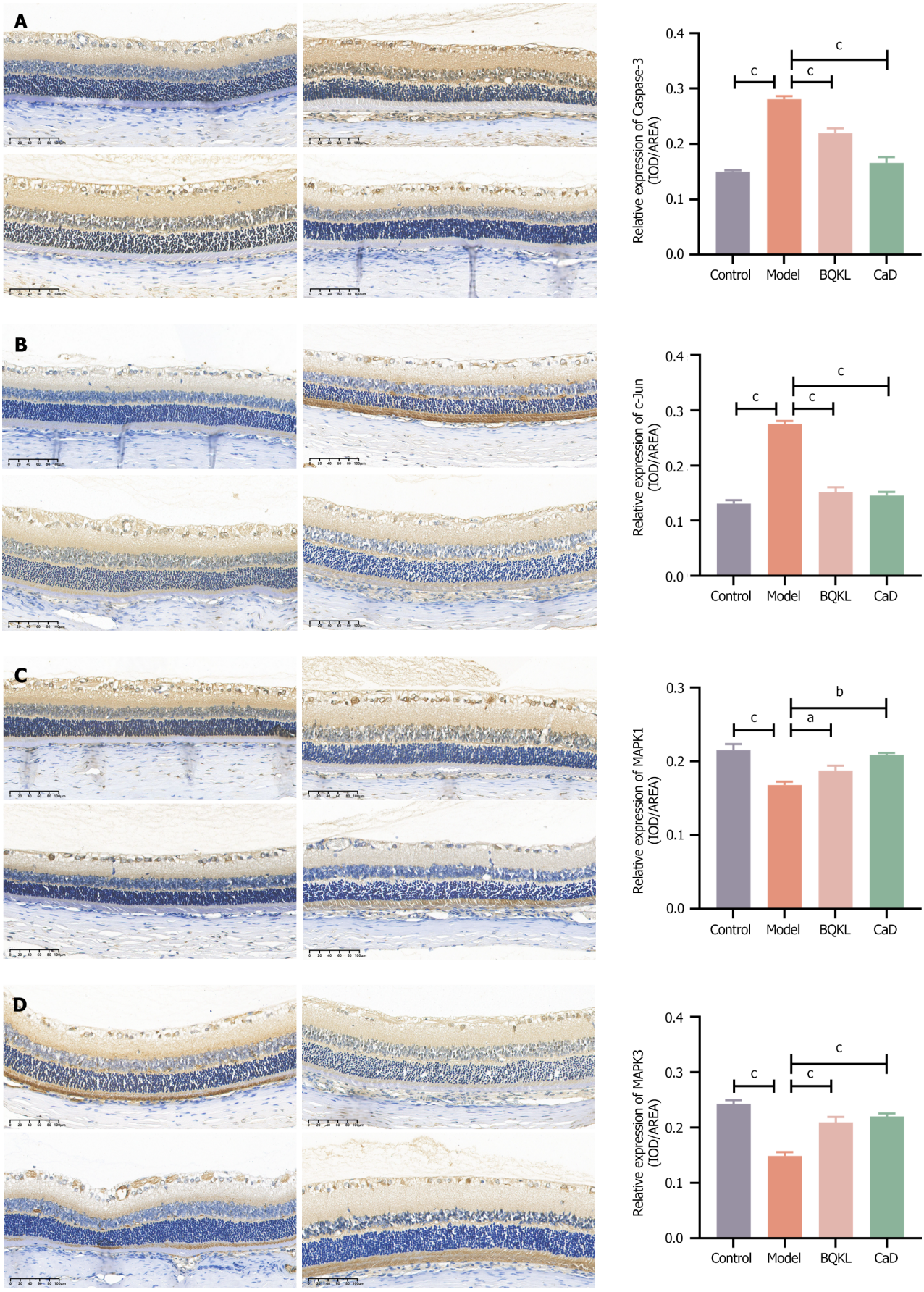

Figure 8 Immunohistochemical results of retinal tissue from different rat models. A: Immunohistochemical detection of Caspase-3; B: Immunohistochemical detection of c-Jun; C: Immunohistochemical detection of MAPK1; D: Immunohistochemical detection of MAPK3 positive expression (200 ×). The sequence from left to right represents the control group, the model group, the Buqing granule group and the calcium dobesilate group. $^{a}P < 0.05$, $^{b}P < 0.01$, $^{c}P <$

0.001. BQKL: Buqing granule; CaD: Calcium dobesilate.

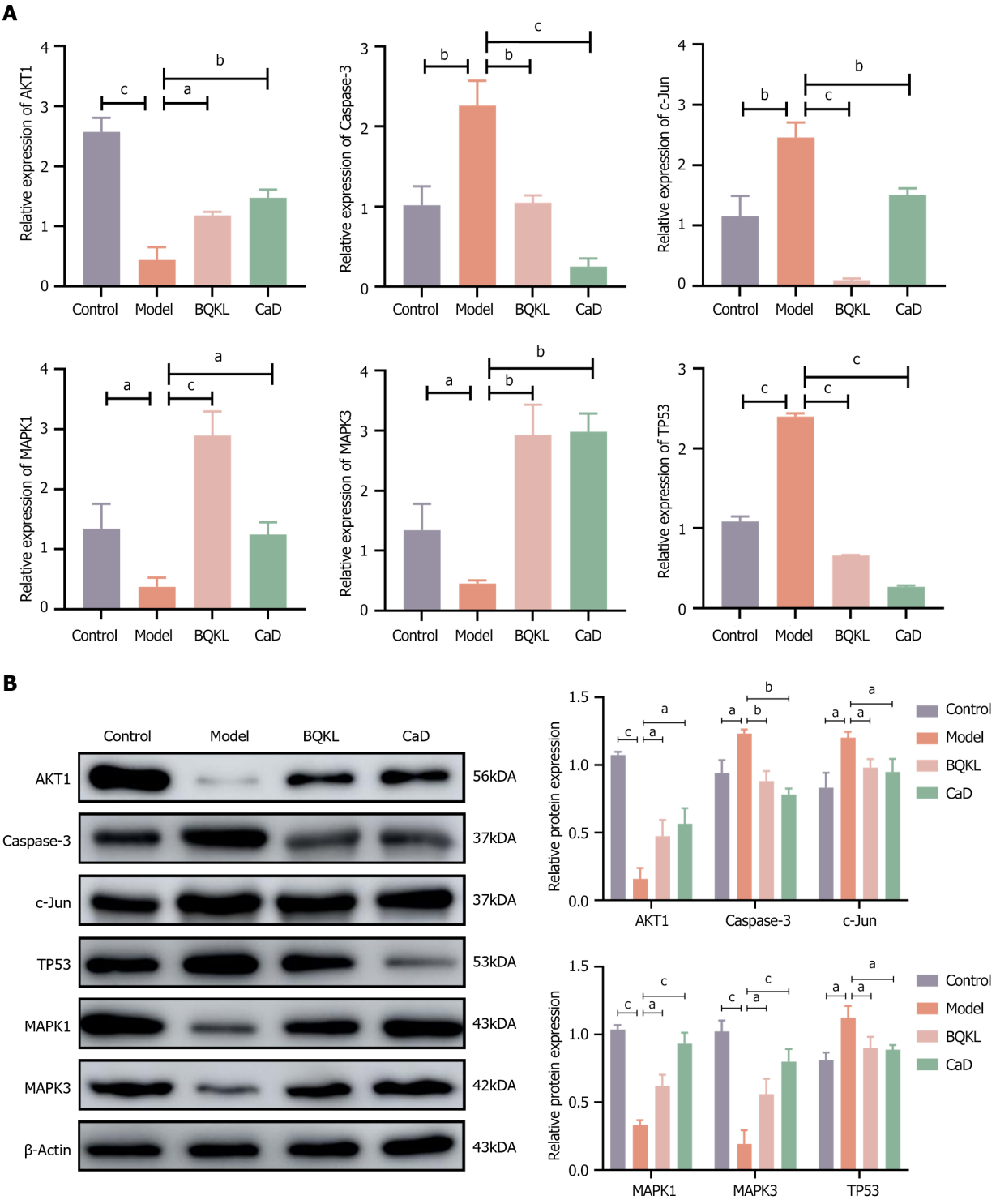

Figure 9 A molecular biological perspective on the role of Buqing granule in the diabetic retinopathy treatment. A: Caspase-3, *AKT1*, *c-Jun*, *TP53*, *MAPK1*, and *MAPK3* mRNA expression levels determined by real-time quantitative reverse transcription-PCR; B: Protein expression levels determined by western blotting. The sequence from left to right represents the control group, the model group, the Buqing granule group and the calcium dobesilate group. $^{a}P < 0.05$, $^{b}P < 0.01$, $^{c}P < 0.001$. BQKL: Buqing granule; CaD: Calcium dobesilate.

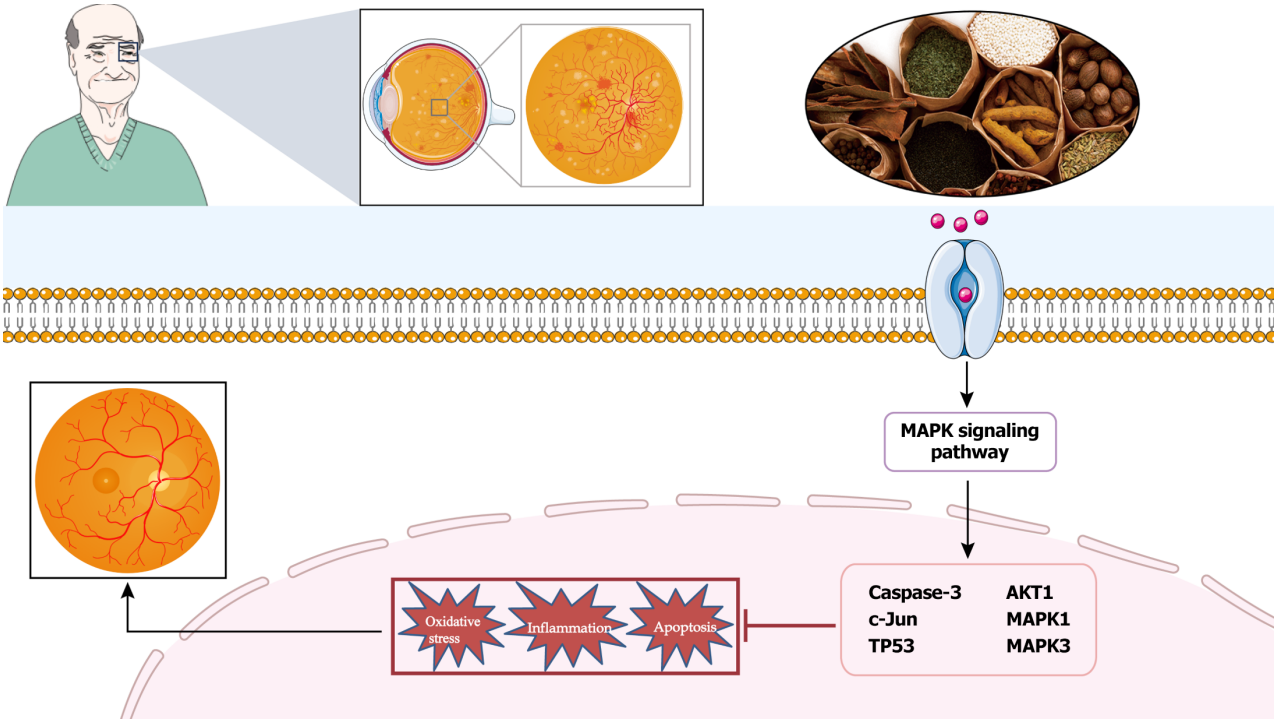

Figure 10 Graphical abstract.

study is only a preliminary investigation of the mechanism of action of BQKL in DR based on network pharmacology and animal experiments, and further experimental validation is required. To effectively investigate the overall gene expression regulation pattern in organisms and explore its connection with disease occurrence and development, we will further analyze the complex genome comprehensively through proteomic metabolomics with high-throughput analysis technology and molecular interactions to provide new avenues for DR diagnosis and treatment.

ACKNOWLEDGEMENTS

We would like to thank the Ningxia Medical University Key Laboratory of Ningxia Minority Medicine Modernization Ministry of Education for providing the experimental platform.

FOOTNOTES

Author contributions: Yang YF conducted most of the experiments, analyzed the data, completed the figure production, and wrote the manuscript; Li XY and Jiang WJ carried out a portion of the experiments and participated in the production of the figures; Jiao TQ carried out part of the experiments and participated in the statistical analysis of the data; Li JQ and Ye MY performed the network pharmacology prediction; Yuan L and Liu Q Critically reviewed and edited the manuscript. Niu Y and Nan Y have played essential and indispensable roles in the experimental design, data interpretation, and manuscript preparation as the co-corresponding authors - Niu Y Secured resources for the study, including animals, equipment, and funding; Nan Y designed and planned the entire research program. As co-corresponding authors, they played a guiding role in the study, helped team members solve problems encountered during the research process, provided professional advice, and promoted the study's progress. All authors approved the final version of the article.

Supported by National Natural Science Foundation of China, No. 81960836; Ningxia Natural Science Foundation, No. 2020AAC03126; and Ningxia Higher Education Scientific Research Project, No. NGY2020045.

Institutional animal care and use committee statement: All animal experiments were approved by the Laboratory Animal Welfare Ethics Committee of the Ningxia Medical University Laboratory Animal Center (No. IACUC-NYLAC-2022-113).

Conflict-of-interest statement: The authors declare that the research was conducted in the absence of any commercial or financial relationships that could be construed as a potential conflict of interest.

Data sharing statement: Dataset available from the corresponding author at 20080011@nxmu.edu.cn.

ARRIVE guidelines statement: The authors have read the ARRIVE guidelines, and the manuscript was prepared and revised according to the ARRIVE guidelines.

Country of origin: China

ORCID number: Ling Yuan 0000-0003-2838-0976; Yang Niu 0000-0001-7778-1560; Yi Nan 0000-0002-5511-9266.

S-Editor: Li L
L-Editor: A
P-Editor: Chen YX

REFERENCES

1 **Liu Y**, Wu N. Progress of Nanotechnology in Diabetic Retinopathy Treatment. *Int J Nanomedicine* 2021; **16**: 1391-1403 [PMID: 33658779 DOI: 10.2147/IJN.S294807]
2 **Cheung N**, Mitchell P, Wong TY. Diabetic retinopathy. *Lancet* 2010; **376**: 124-136 [PMID: 20580421 DOI: 10.1016/S0140-6736(09)62124-3]
3 **Wang W**, Lo ACY. Diabetic Retinopathy: Pathophysiology and Treatments. *Int J Mol Sci* 2018; **19** [PMID: 29925789 DOI: 10.3390/ijms19061816]
4 **Lu Y**, Pan X, Yuan L, Niu Y, Nan Y. Effect of Buqing Granule on Early and Middle Stage Diabetic Cataract in db/db Mice. *Genomics Appl Biol* 2021; **40**: 3330-3336 [DOI: 10.13417/j.gab.040.003330]
5 **Yu Y**, Feng Z, Zhao X, Niu Y. [Clinical observation on 35 cases of immature age-related cataract treated with Buqing soup]. *Ningxia Yike Daxue Xuebao* 2011; **33**: 496-497
6 **Fu H**, Li W, Weng Z, Huang Z, Liu J, Mao Q, Ding B. Water extract of cacumen platycladi promotes hair growth through the Akt/GSK3β/β-catenin signaling pathway. *Front Pharmacol* 2023; **14**: 1038039 [PMID: 36891275 DOI: 10.3389/fphar.2023.1038039]
7 **Gan X**, Shu Z, Wang X, Yan D, Li J, Ofaim S, Albert R, Li X, Liu B, Zhou X, Barabási AL. Network medicine framework reveals generic herb-symptom effectiveness of traditional Chinese medicine. *Sci Adv* 2023; **9**: eadh0215 [PMID: 37889962 DOI: 10.1126/sciadv.adh0215]
8 **Ru J**, Li P, Wang J, Zhou W, Li B, Huang C, Li P, Guo Z, Tao W, Yang Y, Xu X, Li Y, Wang Y, Yang L. TCMSP: a database of systems pharmacology for drug discovery from herbal medicines. *J Cheminform* 2014; **6**: 13 [PMID: 24735618 DOI: 10.1186/1758-2946-6-13]
9 **Pan S**, Hu B, Sun J, Yang Z, Yu W, He Z, Gao X, Song J. Identification of cross-talk pathways and ferroptosis-related genes in periodontitis and type 2 diabetes mellitus by bioinformatics analysis and experimental validation. *Front Immunol* 2022; **13**: 1015491 [PMID: 36248844 DOI: 10.3389/fimmu.2022.1015491]
10 **Amberger JS**, Bocchini CA, Schiettecatte F, Scott AF, Hamosh A. OMIM.org: Online Mendelian Inheritance in Man (OMIM®), an online catalog of human genes and genetic disorders. *Nucleic Acids Res* 2015; **43**: D789-D798 [PMID: 25428349 DOI: 10.1093/nar/gku1205]
11 **Zhou Y**, Zhang Y, Zhao D, Yu X, Shen X, Zhou Y, Wang S, Qiu Y, Chen Y, Zhu F. TTD: Therapeutic Target Database describing target druggability information. *Nucleic Acids Res* 2024; **52**: D1465-D1477 [PMID: 37713619 DOI: 10.1093/nar/gkad751]
12 **Mitra-Ghosh T**, Callisto SP, Lamba JK, Remmel RP, Birnbaum AK, Barbarino JM, Klein TE, Altman RB. PharmGKB summary: lamotrigine pathway, pharmacokinetics and pharmacodynamics. *Pharmacogenet Genomics* 2020; **30**: 81-90 [PMID: 32187155 DOI: 10.1097/FPC.0000000000000397]
13 **Barrett T**, Wilhite SE, Ledoux P, Evangelista C, Kim IF, Tomashevsky M, Marshall KA, Phillippy KH, Sherman PM, Holko M, Yefanov A, Lee H, Zhang N, Robertson CL, Serova N, Davis S, Soboleva A. NCBI GEO: archive for functional genomics data sets--update. *Nucleic Acids Res* 2013; **41**: D991-D995 [PMID: 23193258 DOI: 10.1093/nar/gks1193]
14 **Heberle H**, Meirelles GV, da Silva FR, Telles GP, Minghim R. InteractiVenn: a web-based tool for the analysis of sets through Venn diagrams. *BMC Bioinformatics* 2015; **16**: 169 [PMID: 25994840 DOI: 10.1186/s12859-015-0611-3]
15 **Szklarczyk D**, Gable AL, Nastou KC, Lyon D, Kirsch R, Pyysalo S, Doncheva NT, Legeay M, Fang T, Bork P, Jensen LJ, von Mering C. The STRING database in 2021: customizable protein-protein networks, and functional characterization of user-uploaded gene/measurement sets. *Nucleic Acids Res* 2021; **49**: D605-D612 [PMID: 33237311 DOI: 10.1093/nar/gkaa1074]
16 **Zhang J**, Zhou Y, Ma Z. Multi-target mechanism of Tripteryguim wilfordii Hook for treatment of ankylosing spondylitis based on network pharmacology and molecular docking. *Ann Med* 2021; **53**: 1090-1098 [PMID: 34259096 DOI: 10.1080/07853890.2021.1918345]
17 **Kim S**. Getting the most out of PubChem for virtual screening. *Expert Opin Drug Discov* 2016; **11**: 843-855 [PMID: 27454129 DOI: 10.1080/17460441.2016.1216967]
18 **Rubach P**, Zajac S, Jastrzebski B, Sulkowska JI, Sułkowski P. Genus for biomolecules. *Nucleic Acids Res* 2020; **48**: D1129-D1135 [PMID: 31584078 DOI: 10.1093/nar/gkz845]
19 **Chen M**, Lv H, Gan J, Ren J, Liu J. Tang Wang Ming Mu Granule Attenuates Diabetic Retinopathy in Type 2 Diabetes Rats. *Front Physiol* 2017; **8**: 1065 [PMID: 29311988 DOI: 10.3389/fphys.2017.01065]
20 **Liang WJ**, Yang HW, Liu HN, Qian W, Chen XL. HMGB1 upregulates NF-kB by inhibiting IKB-α and associates with diabetic retinopathy. *Life Sci* 2020; **241**: 117146 [PMID: 31816325 DOI: 10.1016/j.lfs.2019.117146]
21 **Deng ZH**, Niu Y, Wang R, Fan QY, Lang S. [Experimental Study on Protection and Treatment of Galactose Cataract by Buqing Granules]. *Zhongguo Shiyan Fangjixue Zazhi* 2013; **19**: 205-208
22 **Pang B**, Li M, Song J, Li QW, Wang J, Di S, Tong XL, Ni Q. Luo Tong formula attenuates retinal inflammation in diabetic rats *via* inhibition of the p38MAPK/NF-κB pathway. *Chin Med* 2020; **15**: 5 [PMID: 31956338 DOI: 10.1186/s13020-019-0284-3]
23 **Liu Y**, Chen J, Liang H, Cai Y, Li X, Yan L, Zhou L, Shan L, Wang H. Human umbilical cord-derived mesenchymal stem cells not only ameliorate blood glucose but also protect vascular endothelium from diabetic damage through a paracrine mechanism mediated by MAPK/ERK signaling. *Stem Cell Res Ther* 2022; **13**: 258 [PMID: 35715841 DOI: 10.1186/s13287-022-02927-8]

24 **Wang X**, Pan J, Liu H, Zhang M, Liu D, Lu L, Tian J, Liu M, Jin T, An F. AIM2 gene silencing attenuates diabetic cardiomyopathy in type 2 diabetic rat model. *Life Sci* 2019; **221**: 249-258 [PMID: 30790610 DOI: 10.1016/j.lfs.2019.02.035]

25 **Sun HH**, Chai XL, Li HL, Tian JY, Jiang KX, Song XZ, Wang XR, Fang YS, Ji Q, Liu H, Hao GM, Wang W, Han J. Fufang Xueshuantong alleviates diabetic retinopathy by activating the PPAR signalling pathway and complement and coagulation cascades. *J Ethnopharmacol* 2021; **265**: 113324 [PMID: 32890714 DOI: 10.1016/j.jep.2020.113324]

26 **Ma X**, Nan Y, Huang C, Li X, Yang Y, Jiang W, Ye M, Liu Q, Niu Y, Yuan L. Expression of αA-crystallin (CRYAA) in vivo and in vitro models of age-related cataract and the effect of its silencing on HLEB3 cells. *Aging (Albany NY)* 2023; **15**: 4498-4509 [PMID: 37253645 DOI: 10.18632/aging.204754]

27 **Hou Y**, Fan F, Xie N, Zhang Y, Wang X, Meng X. Rhodiola crenulata alleviates hypobaric hypoxia-induced brain injury by maintaining BBB integrity and balancing energy metabolism dysfunction. *Phytomedicine* 2024; **128**: 155529 [PMID: 38503156 DOI: 10.1016/j.phymed.2024.155529]

28 **Liang H**, Ren Y, Huang Y, Xie X, Zhang M. Treatment of diabetic retinopathy with herbs for tonifying kidney and activating blood circulation: A review of pharmacological studies. *J Ethnopharmacol* 2024; **328**: 118078 [PMID: 38513781 DOI: 10.1016/j.jep.2024.118078]

29 **Suganya N**, Dornadula S, Chatterjee S, Mohanram RK. Quercetin improves endothelial function in diabetic rats through inhibition of endoplasmic reticulum stress-mediated oxidative stress. *Eur J Pharmacol* 2018; **819**: 80-88 [PMID: 29169872 DOI: 10.1016/j.ejphar.2017.11.034]

30 **Kahksha**, Alam O, Al-Keridis LA, Khan J, Naaz S, Alam A, Ashraf SA, Alshammari N, Adnan M, Beg MA. Evaluation of Antidiabetic Effect of Luteolin in STZ Induced Diabetic Rats: Molecular Docking, Molecular Dynamics, In Vitro and In Vivo Studies. *J Funct Biomater* 2023; **14** [PMID: 36976050 DOI: 10.3390/jfb14030126]

31 **Alshehri AS**. Kaempferol attenuates diabetic nephropathy in streptozotocin-induced diabetic rats by a hypoglycaemic effect and concomitant activation of the Nrf-2/Ho-1/antioxidants axis. *Arch Physiol Biochem* 2023; **129**: 984-997 [PMID: 33625930 DOI: 10.1080/13813455.2021.1890129]

32 **Choudhary SP**, Tran LS. Phytosterols: perspectives in human nutrition and clinical therapy. *Curr Med Chem* 2011; **18**: 4557-4567 [PMID: 21864283 DOI: 10.2174/092986711797287593]

33 **Babu S**, Jayaraman S. An update on β-sitosterol: A potential herbal nutraceutical for diabetic management. *Biomed Pharmacother* 2020; **131**: 110702 [PMID: 32882583 DOI: 10.1016/j.biopha.2020.110702]

34 **Wang J**, Huang M, Yang J, Ma X, Zheng S, Deng S, Huang Y, Yang X, Zhao P. Anti-diabetic activity of stigmasterol from soybean oil by targeting the GLUT4 glucose transporter. *Food Nutr Res* 2017; **61**: 1364117 [PMID: 28970778 DOI: 10.1080/16546628.2017.1364117]

35 **Kang Q**, Yang C. Oxidative stress and diabetic retinopathy: Molecular mechanisms, pathogenetic role and therapeutic implications. *Redox Biol* 2020; **37**: 101799 [PMID: 33248932 DOI: 10.1016/j.redox.2020.101799]

36 **Kanan Y**, Hackett SF, Taneja K, Khan M, Campochiaro PA. Oxidative stress-induced alterations in retinal glucose metabolism in Retinitis Pigmentosa. *Free Radic Biol Med* 2022; **181**: 143-153 [PMID: 35134532 DOI: 10.1016/j.freeradbiomed.2022.01.032]

37 **Liu H**, Stepicheva NA, Ghosh S, Shang P, Chowdhury O, Daley RA, Yazdankhah M, Gupta U, Hose SL, Valapala M, Fitting CS, Strizhakova A, Shan Y, Feenstra D, Sahel JA, Jayagopal A, Handa JT, Zigler JS Jr, Fort PE, Sodhi A, Sinha D. Reducing Akt2 in retinal pigment epithelial cells causes a compensatory increase in Akt1 and attenuates diabetic retinopathy. *Nat Commun* 2022; **13**: 6045 [PMID: 36229454 DOI: 10.1038/s41467-022-33773-0]

38 **Wu W**, Xie Z, Zhang Q, Ma Y, Bi X, Yang X, Li B, Chen J. Hyperoside Ameliorates Diabetic Retinopathy *via* Anti-Oxidation, Inhibiting Cell Damage and Apoptosis Induced by High Glucose. *Front Pharmacol* 2020; **11**: 797 [PMID: 32547397 DOI: 10.3389/fphar.2020.00797]

39 **Zhao Y**, Sun H, Li X, Zha Y, Hou W. Hydroxysafflor yellow A attenuates high glucose-induced pancreatic β-cells oxidative damage *via* inhibiting JNK/c-jun signaling pathway. *Biochem Biophys Res Commun* 2018; **505**: 353-359 [PMID: 30249395 DOI: 10.1016/j.bbrc.2018.09.036]

40 **Blasiak J**, Chojnacki J, Szczepanska J, Fila M, Chojnacki C, Kaarniranta K, Pawlowska E. Epigallocatechin-3-Gallate, an Active Green Tea Component to Support Anti-VEGFA Therapy in Wet Age-Related Macular Degeneration. *Nutrients* 2023; **15** [PMID: 37571296 DOI: 10.3390/nu15153358]

41 **Kuang L**, You Y, Qi J, Chen J, Zhou X, Ji S, Cheng J, Kwan HY, Jiang P, Sun X, Su M, Wang M, Chen W, Luo R, Zhao X, Zhou L. Qi-dan-dihuang decoction ameliorates renal fibrosis in diabetic rats *via* p38MAPK/AKT/mTOR signaling pathway. *Environ Toxicol* 2024; **39**: 3481-3499 [PMID: 38456329 DOI: 10.1002/tox.24179]

42 **Chu L**, Wang C, Zhou H. Inflammation mechanism and anti-inflammatory therapy of dry eye. *Front Med (Lausanne)* 2024; **11**: 1307682 [PMID: 38420354 DOI: 10.3389/fmed.2024.1307682]

43 **Wang H**, Su X, Zhang QQ, Zhang YY, Chu ZY, Sun ZH, Zhang JL, Tang YF. Cystic Fibrosis Transmembrane Conductance Regulator Attenuates Oxidative Stress-Induced Injury in Diabetic Retinopathy Rats. *Curr Eye Res* 2023; **48**: 416-424 [PMID: 36476257 DOI: 10.1080/02713683.2022.2156548]

Published by **Baishideng Publishing Group Inc**
7041 Koll Center Parkway, Suite 160, Pleasanton, CA 94566, USA
Telephone: +1-925-3991568
E-mail: office@baishideng.com
Help Desk: https://www.f6publishing.com/helpdesk
https://www.wjgnet.com